

EPR of Gd^{3+} in a Single Crystal of Thorium disulfide (ThS_2)

G. Amoretti, D. C. Giori, and V. Varacca

Gruppo Nazionale di Struttura della Materia del Consiglio Nazionale delle Ricerche
and Istituto di Fisica dell'Università, Parma, Italy

Z. Naturforsch. **36a**, 1163–1168 (1981); received September 7, 1981

In this paper we report the experimental angular behaviour of the EPR spectra for a single crystal of Thorium disulfide (ThS_2) doped with Gd^{3+} at very low concentration (of the order of 10 p.p.m.). The experimental data are interpreted in terms of a spin Hamiltonian which reflects the crystal field symmetry at the Th site, that is monoclinic C_s , and therefore shows that the doping ions enter substitutionally without lowering the site symmetry. The low symmetry and the unusually large values of the crystal field parameters b_2^0 and b_2^2 have made it necessary to use a numerical fitting procedure, starting from the exact numerical diagonalization of the energy matrix for any given direction of the static magnetic field.

Introduction

The interpretation of the crystal field effects on S-state ions is still an open problem and any new and accurate experimental result can contribute to a better understanding of the subject.

In a preceding paper [1], we have reported the EPR study on a Gd^{3+} doped single crystal of Thorium oxysulfide (ThOS). Following this line of research, we present in this work the results of the EPR study on a Gd^{3+} doped single crystal of Thorium disulfide (ThS_2).

Both ThOS and ThS_2 have typical structures of many other dichalcogenides of light actinide elements, so that the study of Thorium compounds can be considered also as preliminary to a systematics on those compounds, more significant in the actinide research field.

ThS_2 , contrary to ThOS , shows a low symmetry at the Th site (point group C_s) and, moreover, a very large zero-field splitting, larger than that usually found in crystals of the same structure [2–5]. Therefore, the usual perturbative procedures give very poor results in calculating the spin Hamiltonian parameters, at least for microwave quanta in the X-band frequency range. It is thus necessary to carry out a numerical fitting of the experimental spectra. This is complicated by the large number of parameters required to take into account the low symmetry of the crystal field: many conditions are to be fulfilled and therefore many experimental values must be used. In particular, transitions not

in the directions of the principal axes of the crystal field must be considered to obtain a good fitting of the off-diagonal elements of the Hamiltonian, which are responsible for the asymmetry of the spectra around the principal axes in the reflection plane.

Another interesting feature of compounds like ThOS and ThS_2 is that they may be more suitable for the application of the superposition model [6] than the isostructural ionic compounds, e.g. BaFCl [7] and BaCl_2 [5], owing to the more covalent character of the bonding with the chalcogenides ligands. In particular, as regards ThS_2 , it is to be noted that the large number of crystal field parameters and the spread of the ligand distances, shown by this compound, lead to very restrictive conditions for that model. Therefore, the present results can be very significant for a check of the consistency of the model itself, as will be discussed in a subsequent paper.

Experiment

The single crystal of ThS_2 was grown at the European Institute for Transuranium Elements, Karlsruhe, Federal Republic of Germany, by the method already described [1]. The crystal belongs to the orthorhombic group (space group $P_{mn} - D_{2h}^{16}$), with lattice parameters [8] $a = 4.259 \pm 0.002 \text{ \AA}$, $b = 7.249 \pm 0.003 \text{ \AA}$, $c = 8.600 \pm 0.003 \text{ \AA}$.

The unit cell contains four formula units. The positions of the four thorium and of the eight sulphur ions are given, in fractional coordinates, in [8].

The situation is sketched in Fig. 1, which shows the projection on the bc plane of the structure of

Reprint requests to Prof. Dr. G. Amoretti, Istituto di Fisica dell'Università, Via M. D'Azeglio 85, I-43100 Parma.

0340-4811 / 81 / 1100-1163 \$ 01.00/0. — Please order a reprint rather than making your own copy.



Dieses Werk wurde im Jahr 2013 vom Verlag Zeitschrift für Naturforschung in Zusammenarbeit mit der Max-Planck-Gesellschaft zur Förderung der Wissenschaften e.V. digitalisiert und unter folgender Lizenz veröffentlicht: Creative Commons Namensnennung-Keine Bearbeitung 3.0 Deutschland Lizenz.

Zum 01.01.2015 ist eine Anpassung der Lizenzbedingungen (Entfall der Creative Commons Lizenzbedingung „Keine Bearbeitung“) beabsichtigt, um eine Nachnutzung auch im Rahmen zukünftiger wissenschaftlicher Nutzungsformen zu ermöglichen.

This work has been digitalized and published in 2013 by Verlag Zeitschrift für Naturforschung in cooperation with the Max Planck Society for the Advancement of Science under a Creative Commons Attribution-NoDerivs 3.0 Germany License.

On 01.01.2015 it is planned to change the License Conditions (the removal of the Creative Commons License condition "no derivative works"). This is to allow reuse in the area of future scientific usage.

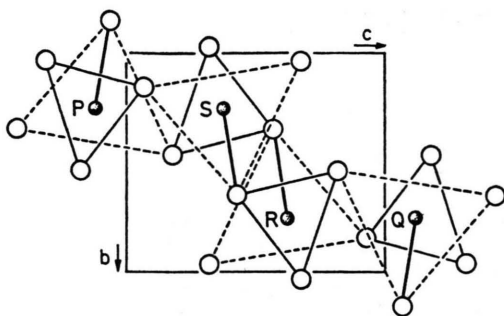


Fig. 1. Projection of the structure of ThS_2 on the bc plane. The coordinates of the units Q and S have been translated by a lattice distance along both axes, with respect to those of Ref. [8], to show the situation in a more compact form.

ThS_2 . Each Th^{4+} is surrounded by nine sulphurs (Table 1) and the point symmetry at the Th site is C_s , with (bc) as reflection plane. From the symmetry of the spectra, we can deduce that the Gd^{3+} ions enter substitutionally in the host matrix. In fact, the EPR spectra in the bc plane consist of two distinct families of resonance curves (each of which can be obtained from the other by reflection through the b or the c axis), according to the fact that the four units of Fig. 1 are magnetically equivalent in pairs. Therefore, it does not seem likely that the charge compensation for the smaller positive charge of Gd^{3+} occurs at short distance from the Gd^{3+} ion itself. In fact, a nearby charge compensator (e.g. a next nearest neighbour S^{2-} vacancy) would perturb the symmetry of the crystal field, unless it should lie exactly on the bc plane. Moreover, it should always be in the same position with respect to the Gd^{3+} ion, otherwise it would give rise to a splitting or a broadening of the line, which we have not observed [3]. The linewidth was in fact about 15 G and no hyperfine splitting was resolved.

Table 1. Fractional coordinates of the ions of the unit labelled P in Figure 1. The ligands are ordered by increasing distance from the central Th^{4+} ion.

| | X/a | Y/b | Z/c |
|------------|-----------|--------|--------|
| Th | 1/4 | 0.250 | -0.125 |
| S_1 | 1/4 | 0.350 | -0.432 |
| $S_{2,2'}$ | -1/4, 3/4 | 0.150 | 0.068 |
| S_3 | 1/4 | -0.150 | -0.068 |
| $S_{4,4'}$ | -1/4, 3/4 | 0.535 | -0.180 |
| S_5 | 1/4 | 0.465 | 0.180 |
| $S_{6,6'}$ | -1/4, 3/4 | 0.035 | -0.320 |

From the intensity of the spectra we can infer that the doping ions enter in a final proportion of the order of 10 p.p.m.

The EPR spectra have been recorded at room temperature by means of a X-band Varian 9E-line spectrometer, equipped with an E233 rotating cavity. The values of the static magnetic field, necessary to the fitting procedure, were measured by a field controller [1] with an accuracy better than 0.2 G, while a sample of DPPH was placed into the cavity to monitor the microwave frequency. The ultimate mean accuracy can be estimated to lie within ± 5 G, owing principally to the fact that for the lines at higher magnetic field (in the directions near the crystal field axes) the angular setting of the magnetic field is very critical.

To have the complete angular variation of the spectra, the remaining resonance fields were measured directly on the recorded spectra, and therefore the accuracy is much lower for such lines, namely ± 20 G. The angular variation of the spectra was followed in the bc and ac crystallographic planes. The direction of maximum overall splitting was found at $20.7 \pm 0.5^\circ$ from the c axis, in the bc plane.

Spin Hamiltonian and Fitting Procedure

The spin Hamiltonian, in the case of C_s point symmetry, can be written [9–11]

$$\mathcal{H} = \mu_B (g_x H_x S_x + g_y H_y S_y + g_z H_z S_z) + \sum_{\substack{n=2 \\ (\text{even})}}^6 \sum_{m=0}^n B_n^m O_n^m, \quad (1)$$

where μ_B is the Bohr magneton.

As usual, we have assumed that the principal axes of the g -tensor are coincident with those of the fine structure. This is not a restrictive hypothesis, because the g values are isotropic within the experimental errors, as expected. The y axis of the fine structure has been chosen coincident with the crystallographic a axis. Owing to the non coincidence of the extrema of the angular dependence of the resonance fields [12], the direction of the z axis, in the bc plane, has been determined according to the condition $B_2^1 = 0$ [2, 11, 13]. Taking into account that the low symmetry effects are small, we have initially assumed the direction of the z axis along that of maximum overall splitting [13]. From

the best fitting of the experimental spectra, discussed in the following, under the quoted condition for B_2^1 , the z axis results to lie at an angle of 20.35° from the c axis in the bc plane (Fig. 2), coincident, within experimental error, with the direction of maximum splitting and therefore supporting the initial assumption. With this choice of the reference frame, B_2^0 results to be the largest parameter. Other authors [2–5] have preferred to use a different expression of the Hamiltonian (1), with the x axis along the direction of maximum splitting and the z axis along the crystallographic a axis. In this case, the off-diagonal parameter B_2^2 is the largest one. However, the two assumptions are completely equivalent and the two sets of parameters can be related by suitable transformations [9].

From the angular variation of the spectra, shown in Figs. 2 and 3, and from the behaviour of the energy levels as functions of the magnetic field (Figs. 4 and 5), it appears that the usual perturbative treatment [1, 11] can not be successfully applied to evaluate the spin Hamiltonian parameters. In fact, the large splitting and the low symmetry, which is responsible for the large number of off-diagonal crystal field parameters and therefore for the asymmetric behaviour of the resonance lines in the bc plane (Fig. 2), make it necessary to adopt a numerical fitting procedure. In this way, it was possible to fit simultaneously the experimental values of the resonance fields for a number of different orientations, sufficient to obtain the values of all the parameters of (1). The method [14] is consistent with the usual procedure in which one assumes the z' quantization axis along the direction of the static magnetic field. In this way, the perturbation theory can be applied to the higher field lines of the spectra, to obtain reasonable starting values of the most important parameters, to be used in the fitting procedure. Moreover, the asymptotic eigenstates can be simply labelled by the z' component of the effective spin, whichever direction the static magnetic field assumes in the rotation plane. This makes easier to follow the behaviour of the eigenvalues as functions both of the field modulus and of the field direction, by means of a continuity criterion for the corresponding eigenstates. This is particularly useful to identify the allowed transitions in the low field zone, where the effects of crossing and non crossing of the energy levels become important [6]. The method, which

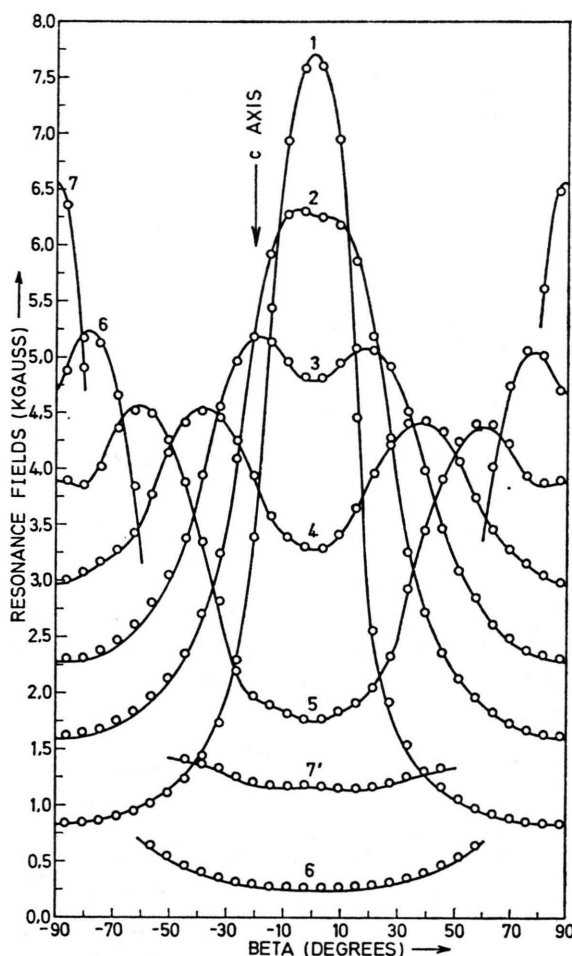


Fig. 2. Angular variation of the EPR spectra in the bc plane for one of the two inequivalent units. Curves: calculated values; dots: experimental values. For the labelling of the transitions see also Figure 4.

can be applied to the case of monoclinic or higher symmetry and for any value of the effective spin, is based on the energy matrix written in a very general form, that is for the static magnetic field \mathbf{H} along any fixed direction, defined by the Euler angles $(\alpha, \beta, 0)$ [15, 16]. In this case, within the $S=7/2$ manifold, the Hamiltonian (1) can be written as

$$\mathcal{H}' = \mu_B g(\alpha, \beta) H_z S_z' + \sum_{\substack{n=2 \\ (\text{even})}}^6 \sum_{m'=0}^n C_n^{m'}(\alpha, \beta) O_n^{m'}, \quad (2)$$

where $g(\alpha, \beta)$ is the g -value in the direction of the field. The coefficients $C_n^{m'}(\alpha, \beta)$ are defined as

$$C_n^0(\alpha, \beta) = \sum_{m=0}^n D_{0m}^n(\beta) \cos(m\alpha) B_n^m, \quad (3a)$$

$$C_n^{m'}(\alpha, \beta) = C_{n+}^{m'}(\alpha, \beta) \pm i C_{n-}^{m'}(\alpha, \beta), \quad m' \neq 0, \quad (3b)$$

where

$$C_{n+}^{m'}(\alpha, \beta) = \sum_{m=0}^n D_{m'm}^{n+}(\beta) \cos(m\alpha) B_n^m \quad (3c)$$

and

$$C_{n-}^{m'}(\alpha, \beta) = \sum_{m=0}^n D_{m'm}^{n-}(\beta) \sin(m\alpha) B_n^m. \quad (3d)$$

The sign to be used in (3b) depends on the states between which the matrix elements of (2) are evaluated [16]. That is, in the element $\langle \mu' | \mathcal{H}' | \mu \rangle$, where μ is the z' component of the effective spin, the top sign must be used for $\mu' < \mu$ and the bottom one for $\mu' > \mu$. D_{0m}^n and $D_{m'm}^{\pm n}$ are the coefficients defined by Baker and Williams [16].

While the Zeeman term is always diagonal, the contributions to the energy matrix of the crystal field terms can be written in terms of the matrix elements

$$\mu P_{m'} = \sum_{\substack{n=2 \\ (\text{even})}}^6 \langle \mu - m' | O_n^{m'} | \mu \rangle C_n^{m'}(\alpha, \beta), \quad \mu > 0, \quad (4a)$$

$$\mu Q_{m'} = \sum_{\substack{n=2 \\ (\text{even})}}^6 \langle \mu | O_n^{m'} | \mu + m' \rangle C_n^{m'}(\alpha, \beta), \quad \mu < 0, \quad (4b)$$

which connect states with a difference equal to m' in the z' component of the spin. The matrix elements of the equivalent operators $O_n^{m'}$ are known and tabulated [17, 18] and therefore the matrix elements (4) can be explicitly written as linear combinations of the $C_n^{m'}$'s, which in turn are linear combinations of the B_n^m 's. In this way, the angular behaviour of the EPR spectra can be fitted by a trial and error procedure, starting either from a perturbative treatment or from the exact diagonalization of the energy matrix at the experimental values of the resonance fields, for all the required directions. Therefore, the g -values and the reduced parameters b_n^m (related as usual [1, 6] to the B_n^m 's) were calculated as follows.

The field values were accurately measured along six directions in the bc plane, namely that of maximum splitting, assumed as z axis, the direction at $\pi/2$ from this one, assumed as x axis, and at $\pm 5^\circ$ and $\pm 10^\circ$ from the assumed z axis, in order to take into account the low symmetry effects on the

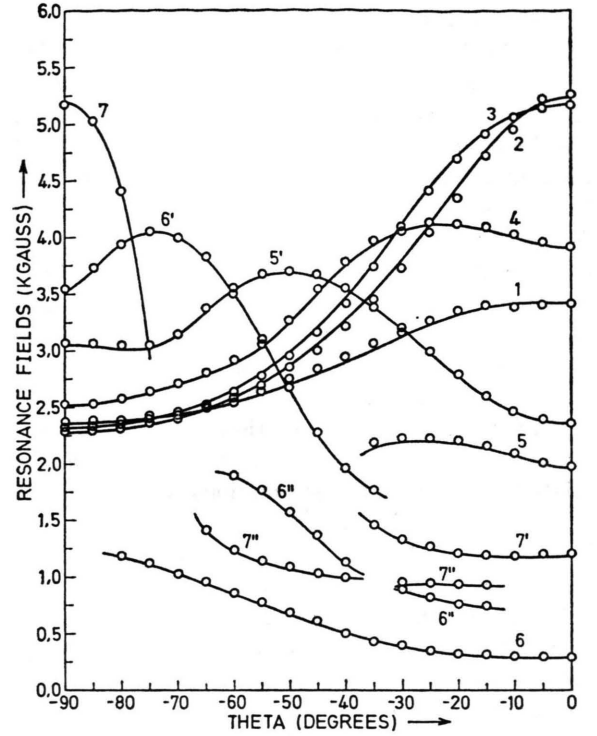


Fig. 3. Angular variation of the EPR spectra in the ac plane. Curves: calculated values; dots: experimental values. The c axis is at 0° .

spectra [13]. From the values along the principal axes it is possible, by a perturbative approach, to obtain the starting values of the largest parameters of even m , while from those in the other directions one can evaluate at least the order of magnitude of the largest odd parameters.

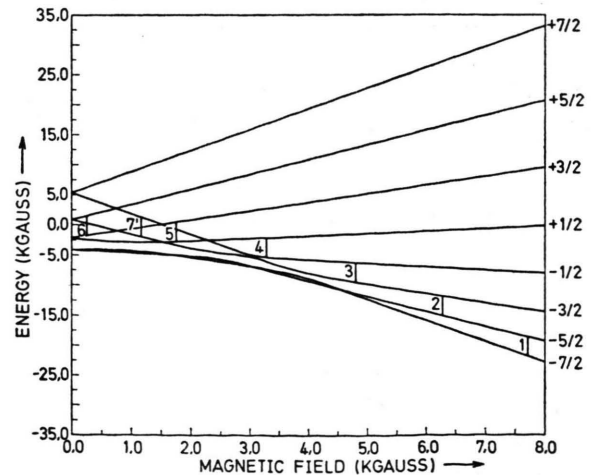


Fig. 4. Energy level scheme for Gd^{3+} in ThS_2 , when $H \parallel z$.

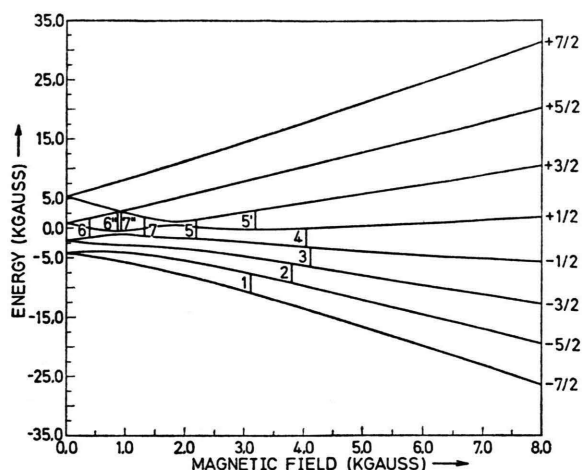


Fig. 5. Energy level scheme for Gd^{3+} in ThS_2 , when \mathbf{H} forms an angle $\theta = -30^\circ$ with the c axis, in the ac plane. (In the figure please read 7' instead of 7.)

With these initial values, the fitting procedure was carried out in cyclic steps. That is, first of all the lowest order parameters b_2^m were varied to fit the experimental values of the resonance fields; then the b_4^m 's, the values of which were successively used to refine the b_2^m 's; finally, the b_6^m 's, until the best fitting was achieved. This is defined by the simultaneous minimum values of the sums of the squares of the differences between the experimental value of the microwave quantum energy and the transition energies calculated for each resonance along the quoted directions.

The problem of identifying unambiguously the $\Delta m = \pm 1$ transitions in the set of levels at a given magnetic field, for each fixed direction, has been bypassed drawing the preliminary diagrams of the energy levels as functions of the magnetic field and calculating the transition probabilities of all the available transitions.

As regards the resulting orientation of the crystal field z axis, it must be noted that a good fitting of the experimental data in the bc plane was already obtained with the initial assumption and the quoted condition $b_2^1 = 0$. Subsequently, the angle between the z and the c axes was slightly varied, always under the condition $b_2^1 = 0$, until the best fitting of the whole angular behaviour was obtained. This occurred for a value of the angle of 20.35° . This result was furthermore supported by the fitting of the angular variation of the spectra in the ac plane (Fig. 3), which did not require any further refinement of the calculated values of the parameters and of the angle.

Results and Discussion

In Table 2 the parameters of the Hamiltonian (1), deduced with the method quoted in the preceding Section, are listed. The error has been estimated for every single parameter as the variation which gives a distinguishable deviation ($1 \div 2$ gauss) from the best fitting values of the energy differences. The average deviation between the measured and calculated resonance fields, along the principal axes of the crystal field, is 10 gauss, with a minimum value of 1 gauss for a line along z and a maximum value of 33 gauss for a line along the x axis. An even better agreement could have been obtained along the axes, but with the result to spoil the fitting in the other directions. We have preferred to choose, as the best set of values for the parameters, the set which allows the best reproduction of the whole angular behaviour of the experimental resonance fields. Figures 2 and 3 show just the comparison between the experimental and the calculated fields in the bc (xz) and ac planes respectively.

To better understand the principal features of the curves in Figs. 2 and 3, the energy level scheme for $\mathbf{H} \parallel z$ is shown in Fig. 4, and the scheme for \mathbf{H} along a particular direction in the ac plane is shown in Figure 5. The characteristic non crossing of the levels can be noted and related to the off-diagonal terms of (1) [6]. In particular, the three largest gaps in the scheme of Fig. 4 are due to the large value of b_2^2 [19]. As a consequence of the gaps, and moreover of the large values of b_2^0 and b_2^2 , some transitions vanish approaching a gap from one side, as the magnetic field rotates in the given plane, and reappear on the other side. This is the case, for example, of the transitions labelled 6 and 7 in

Table 2. Values of the spin Hamiltonian parameters for Gd^{3+} in ThS_2 . b_n^m 's are given in 10^{-4} cm^{-1} .

| | |
|-------------------------|------------------------|
| $g_x = 1.995 \pm 0.002$ | $b_4^0 = -4.0 \pm 0.1$ |
| $g_y = 1.993 \pm 0.002$ | $b_4^1 = 25 \pm 2$ |
| $g_z = 1.994 \pm 0.002$ | $b_4^2 = -4 \pm 1.5$ |
| | $b_4^3 = -125 \pm 15$ |
| | $b_4^4 = -20 \pm 2$ |
| $b_2^0 = 708.0 \pm 0.6$ | $b_6^0 = 0.0 \pm 0.2$ |
| $b_2^1 = 0 \pm 3$ | $b_6^1 = -5 \pm 3$ |
| $b_2^2 = -243 \pm 1$ | $b_6^2 = -6 \pm 3$ |
| | $b_6^3 = -10 \pm 6$ |
| | $b_6^4 = -5 \pm 3$ |
| | $b_6^5 = 0 \pm 15$ |
| | $b_6^6 = -12 \pm 3$ |

Figure 2. In particular, the second one, which corresponds to the transition between the $+7/2$ and the $+5/2$ asymptotic levels, can not be actually connected to a curve around the z axis, because the energy splitting between these levels becomes larger than $\hbar\nu$ near the z axis. Therefore, we have drawn the curve 7', which would correspond to the transition $-7/2 \rightarrow -5/2$ and which can be ideally related to the preceding one as deriving from the "reflection" of the $+5/2$ and $+7/2$ levels at $H=0$. The situation is much more complicated in the ac plane, as shown in Fig. 3 [20]. The curves labelled by the same number can be related to the same pair of asymptotic levels (see Figure 5). Moreover, such labelling is consistent, along the c axis, with that of Figure 2.

We want to point out that the uncertainty on the crystal field parameters b_n^m is smaller, except for b_6^5 , than that previously reported for compounds of low site symmetry [2–5, 9, 13]. The g values are substantially isotropic and slightly larger than in the case of ThOS [1]. This could suggest a smaller spin-orbit coupling with the excited states. On the

other hand, however, this should be in contrast with the large value of the quadrupolar parameter b_2^0 . Such contradiction disappears if one considers the different symmetries and therefore the different contributions of the ligands in the two cases.

Preliminary superposition model [6] calculations on the second degree parameters [21] support the choice of the positive sign for b_2^0 and, therefore, the energy level scheme of Fig. 4 is consistent with this sign, that is with the $\pm 7/2$ doublet highest in energy at zero field.

An experimental attempt to confirm this sign from the intensities of the lines of the spectrum at liquid helium temperature [22] has not given significant results, because ThS_2 seems to undergo a structural phase transition below 10 K. Further studies are going on at present.

Acknowledgements

We wish to thank Prof. P. Sgarabotto, of the Istituto di Strutturistica Chimica, for his assistance in the orientation of the crystal and Mr. B. Valenti for his help in recording the spectra.

- [1] G. Amoretti, D. C. Giori, V. Varacca, J. C. Spirlet, and J. Rebizant, *Phys. Rev. B* **20**, 3573 (1979).
- [2] Q. H. F. Vrehen and J. Volger, *Physica* **31**, 845 (1965).
- [3] H. C. W. Beijerinck and B. Willemsen, *Physica* **47**, 515 (1970).
- [4] B. Willemsen and W. C. Hommels, *Phys. Stat. Sol. (a)* **10**, 183 (1972).
- [5] H. Wever and H. W. den Hartog, *Phys. Stat. Sol. (b)* **70**, 253 (1975).
- [6] D. J. Newman and W. Urban, *Adv. Phys.* **24**, 793 (1975).
- [7] D. Niccolin and H. Bill, *J. Phys. C: Sol. State Phys.* **11**, 4803 (1978).
- [8] W. H. Zachariasen, *Acta Crystallogr.* **2**, 291 (1949).
- [9] V. B. Kravchenko, I. A. Gavrilov, A. T. Sobolev, O. F. Dudnik, and B. I. Kryuchkov, *Sov. Phys. Sol. State* **11**, 2898 (1970).
- [10] U. L. Meil'man and I. A. Gavrilov, *Sov. Phys. Sol. State* **11**, 628 (1969).
- [11] H. A. Buckmaster and Y. H. Shing, *Phys. Stat. Sol. (a)* **12**, 325 (1972).
- [12] A. B. Roitsin, *Phys. Stat. Sol. (b)* **104**, 11 (1981).
- [13] L. Kratena, K. Zdansky, and V. Sik, *Phys. Stat. Sol.* **28**, 175 (1968).
- [14] G. Amoretti, *Proc. Joint ISMAR-Ampère Int. Conf. (Delft, 1980)*, *Bull. Magn. Res.* **2**, 159 (1981).
- [15] A. R. Edmonds, *Angular Momentum in Quantum Mechanics*, University Press, Princeton 1960.
- [16] J. M. Baker and F. I. B. Williams, *Proc. Phys. Soc. London* **78**, 1340 (1961).
- [17] A. Abragam and B. Bleaney, *Electron Paramagnetic Resonance of Transition Ions*, Clarendon Press, Oxford 1970.
- [18] H. A. Buckmaster, *Canad. J. Phys.* **40**, 1670 (1962).
- [19] These gaps correspond to the repelling points labelled with the numbers 2, 5 and 10 in [6].
- [20] The angular variation in this plane is given on a range of $\pi/2$ only, because the spectrum behaves symmetrically with respect to both a and c axis, as also requested by the transformation properties of the equivalent operators. The angle θ gives the direction of the magnetic field in the ac plane and can be simply related to the Euler angles α and β , which define the generical direction of \mathbf{H} .
- [21] G. Amoretti, D. C. Giori, and V. Varacca, *Proc. Joint ISMAR-Ampère Int. Conf., Delft 1980*, *Bull. Magn. Res.* **2**, 158 (1981).
- [22] J. Rosenthal, R. F. Riley, and U. Ranon, *Phys. Rev.* **177**, 625 (1969).